ACS Sustainable Chemistry & Engineering

Research Article

Cite This: ACS Sustainable Chem. Eng. XXXX, XXX, XXX−XXX

pubs.acs.org/journal/ascecg

Tunable Hydrophobic Eutectic Solvents Based on Terpenes and Monocarboxylic Acids

Mónia A. R. Martins,[†,‡,§,∥] Emanuel A. Crespo,[†,⊥] Paula V. A. Pontes,[∥] Liliana P. Silva,[†] Mark Bülow,[⊥] Guilherme J. Maximo,[∥] Eduardo A. C. Batista,[∥] Christoph Held,[⊥] Simão P. Pinho,[‡,§] and João A. P. Coutinho*[,†]

[†]CICECO − Aveiro Institute of Materials, Department of Chemistry, University of Aveiro, 3810-193 Aveiro, Portugal

[‡]Associate Laboratory LSRE-LCM, Department of Chemical and Biological Technology, Polytechnic Institute of Bragança, 5300-253 Bragança, Portugal

[§]Mountain Research Center − CIMO, Polytechnic Institute of Bragança, 5301-855 Bragança, Portugal

[∥]Faculty of Food Engineering, University of Campinas, 13083-862 Campinas, Brazil

[⊥]Laboratory of Thermodynamics, Department of Biochemical and Chemical Engineering, TU Dortmund, 44227 Dortmund, Germany

S *Supporting Information*

ABSTRACT: Recently, some works claim that hydrophobic deep eutectic solvents could be prepared based on menthol and monocarboxylic acids. Despite of some promising potential applications, these systems were poorly understood, and this work addresses this issue. Here, the characterization of eutectic solvents composed of the terpenes thymol or L(−)-menthol and monocarboxylic acids is studied aiming the design of these solvents. Their solid−liquid phase diagrams were measured by differential scanning calorimetry in the whole composition range, showing that a broader composition range, and not only fixed stoichiometric proportions, can be used as solvents at low temperatures. Additionally, solvent densities and viscosities close to the eutectic compositions were measured, showing low viscosity and lower density than water. The solvatochromic parameters at the eutectic composition were also investigated aiming at better understanding their polarity. The high acidity is mainly provided by the presence of thymol in the mixture, while L(−)-menthol plays the major role on the hydrogen-bond basicity. The measured mutual solubilities with water attest to the hydrophobic character of the mixtures investigated. The experimental solid−liquid phase diagrams were described using the PC-SAFT equation of state that is shown to accurately describe the experimental data and quantify the small deviations from ideality.

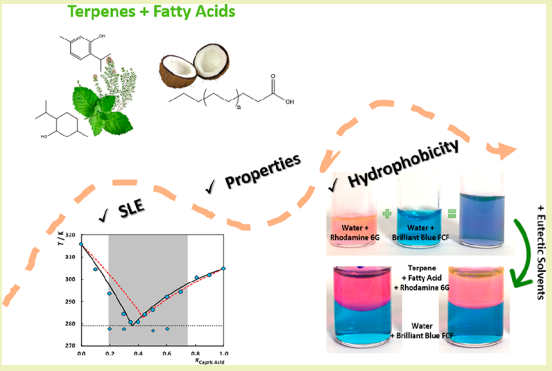

KEYWORDS: *Terpenes, Monocarboxylic acids, SLE, PC-SAFT, Solvatochromic parameters, Densities, Viscosities, Eutectic solvents*

INTRODUCTION

Nowadays, developments in engineering and technology are strongly influenced by the concepts of *green chemistry* and *sustainability*. Within this framework, there is a demand for new ecofriendly solvents able to dissolve a large spectrum of solutes. Currently, one of the most important focuses of research for novel solvents are the eutectic mixtures, particularly the so-called deep eutectic solvents (DES).[1]

Most of the deep eutectic solvents proposed so far were prepared through the combination of materials from renewable resources with nontoxic and biodegradable compounds such as carboxylic acids,[2] polyols, and sugars,[3] with the vast majority being hydrophilic. To the best of our knowledge, only a limited number of works reported hydrophobic eutectic mixtures.[4−7] However, in these studies, the solid−liquid phase diagrams were not characterized despite the relevant information that they can provide on the range of composition and temperature for operating these systems, while the physical−chemical characterization of their properties is also poor.

Because of their very low solubility in water and relatively low price,[8] terpenes appeared as good candidates to prepare sustainable and cheap hydrophobic solvents. Menthol and thymol are monoterpenoids used in various industrial processes and commercial products, and the use of their eutectic mixtures has been investigated. In the pharmaceutical field, mixtures of borneol/menthol[9] and camphor/menthol[10] have been proposed as vehicles for transdermal delivery.[11] Moreover, mixtures of thymol with ibuprofen[12] or meloxicam[11] and of

Received: March 16, 2018
Revised: May 24, 2018
Published: May 29, 2018

DOI: 10.1021/acssuschemeng.8b01203
ACS Sustainable Chem. Eng. XXXX, XXX, XXX−XXX

Table 1. Compounds Description and Their Melting Properties Along with Values from Literature

				T_m/K		$\Delta_m H$/kJ·mol^{-1}	
Compound	Supplier	CAS	Purity wt %[a]	exp.	lit.	exp.	lit.
L(−)-menthol	Acros	2216−51−5	99.7	315.68[b] ± 0.22	315.9[21] 316.7[21]	12.89[b] ± 0.77	12.83[21]
Thymol	Sigma	89−83−8	≥99.5	323.50[b] ± 0.34	323.1[21] 322.8[21]	19.65[b] ± 0.42	17.54[21]
Caprylic acid	Sigma	124−07−2	≥99	288.20[b] ± 0.09	289.50[22]	19.80[b] ± 0.54	21.38[22]
Capric acid	Sigma	334−48−5	99−100	–	304.75[23,b]	–	27.50[23,b]
Lauric acid	Sigma	143−07−7	≥99	–	317.48[23,b]	–	34.69[24,b]
Myristic acid	Sigma	544−63−8	≈95	–	327.03[23,b]	–	45.75[25,b]
Palmitic acid	Aldrich	57−10−3	≥98	–	336.84[23,b]	–	51.02[23,b]
Stearic acid	Merck	57−11−4	≥97	–	343.67[23,b]	–	61.36[23,b]

[a]Declared by the supplier. [b]Melting properties considered in the PC-SAFT modeling.

menthol with ibuprofen,[13] testosterone,[14] lidocaine,[15] or ubiquinone[16] have been investigated as an analgesic, antimicrobial, and anti-inflammatory vehicles.[17] Recently, mixtures of menthol and ibuprofen, benzoic acid, acetylsalicylic acid, or phenylacetic acid were proposed as therapeutic deep eutectic solvents used to design a controlled drug delivery system using supercritical fluid technology[18] and as dissolution enhancers of active pharmaceutical ingredients.[19]

Combining terpenes and carboxylic acids, the menthol-lauric acid mixture was proposed as a hydrophobic DES able to extract indium from aqueous solutions,[7] and hydrophobic mixtures of menthol and naturally occurring acids, namely, pyruvic acid, acetic acid, L-lactic acid, and lauric acid, were applied as solvents in the extraction of caffeine, tryptophan, isophthalic acid, and vanillin.[17] Furthermore, mixtures of DL-menthol with caprylic, capric, and lauric acids were shown to be able to extract up to 80% of neonicotinoids from diluted aqueous solutions.[5]

The main goal of this work is to prepare and characterize eutectic mixtures composed by terpenes and monocarboxylic acids. The terpenes under study are L(−)-menthol and thymol, while as carboxylic acids caprylic, capric, lauric, myristic, palmitic, and stearic acids are used. Solid−liquid phase diagrams of these mixtures are measured in the whole composition range, through differential scanning calorimetry (DSC) and described by the Perturbed Chain-Statistical Associating Fluid Theory (PC-SAFT) equation of state (EoS),[20] a molecular-based approach able to explicitly take into account the association between the different constituents of the eutectic mixtures. Moreover, the densities, viscosities, solvatochromic parameters, and mutual solubilities with water are measured at compositions close to the eutectic point. The experimental liquid densities are also predicted using PC-SAFT.

EXPERIMENTAL SECTION

Chemicals. Information on the studied compounds is summarized in Table 1 and Figure S1. The samples were used as received without further purification. The purity of the terpenes was evaluated by ^{1}H and ^{13}C NMR spectra and GC-MS.

Methods. *Mixtures Preparation.* Binary mixtures of terpene and carboxylic acid were prepared by adding the compounds into glass vessels at different molar ratios in the full composition range, using an analytic balance XP205 (Mettler Toledo, precision = 0.2 mg). The mixtures were melted under stirring on a heating plate until a homogeneous liquid mixture was obtained and then cooled to room temperature. Samples (2−5 mg) were hermetically sealed in aluminum pans and weighed in a microanalytical balance AD6 (PerkinElmer, USA, precision = 0.002 mg). Mixtures were analyzed by NMR spectroscopy at room temperature 48 h after their formation (Figure S2). No differences in the spectra or new NMR signals were observed 48 h after the formation of the systems, showing that esterification did not take place, thus proving the stability of the studied mixtures.

Differential Scanning Calorimetry. The melting points of pure components and their mixtures were determined using a DSC 2920 calorimeter from TA Instruments working at atmospheric pressure and coupled to a cooling system. The equipment was previously calibrated with indium. The analytical procedure was based on a cooling ramp down to 208.15 at 5 K·min^{-1}, followed by a heating ramp up to 10 K above melting at 1 K·min^{-1}. A constant nitrogen flow (purity ≥0.99999 mass fraction) was used as the purge gas to avoid condensation of water at low temperatures. Data were analyzed through the TA Universal Analysis software (TA Instruments), and the melting temperature taken as the peak temperature. At least three cycles of cooling and heating were performed for pure compounds and one cycle for mixtures.

Density and Viscosity. Densities and viscosities were measured at atmospheric pressure and in the temperature range from 278.15 to 373.15 K using an automated SVM 3000 Anton Paar rotational Stabinger viscometer−densimeter (temperature uncertainty: ± 0.02 K; absolute density uncertainty: ± 5 × 10^{-4} g·cm^{-3}; dynamic viscosity relative uncertainty: ± 0.35%).

Kamlet−Taft Solvatochromic Parameters. The solvatochromic parameters π^*, β, and α were measured at 323.15 K by adding very small quantities of the probes *N*,*N*-diethyl-4-nitroaniline, 4-nitroaniline, and pyridine-*N*-oxide, respectively, to the different eutectic mixtures (ca. 500 μL).[26,27] Mixtures were then stirred (Eppendorf Thermomixer Comfort) at 323.15 K and 1400 rpm during 30 min, until complete dissolution. Regarding π^* and β, the longest wavelength absorption band was analyzed using UV−vis spectroscopy (BioTeck Synergy HT microplate reader) at 323.15 K. The α parameter was determined by ^{13}C nuclear magnetic resonance (NMR) spectra, using a Bruker Avance 300 equipment operating at 75 MHz. Deuterium oxide (D_2O) was used as the solvent and trimethylsilyl propanoic acid (TSP) as the internal reference. At least three independent measurements were performed for each parameter and mixture.

Mutual Solubilities. The solubility of water in the eutectic mixtures was evaluated using a Metrohm 831 Karl Fischer, whereas the solubility of thymol in the water-rich phase was measured using a methodology previously detailed elsewhere.[8,28]

Theoretical Framework. *Solid−Liquid Equilibria.* Considering that the solid phases crystallize independently as pure solids and neglecting the effect of temperature on the heat capacities, the solubility of a solid in a liquid solvent can be described using the following expression:[29]

$$\ln(x_i\gamma_i^l) = \frac{\Delta_m H}{R}\left(\frac{1}{T_m} - \frac{1}{T}\right) + \frac{\Delta_m C_p}{R}\left(\frac{T_m}{T} - \ln\frac{T_m}{T} - 1\right) \quad (1)$$

DOI: 10.1021/acssuschemeng.8b01203
ACS Sustainable Chem. Eng. XXXX, XXX, XXX−XXX

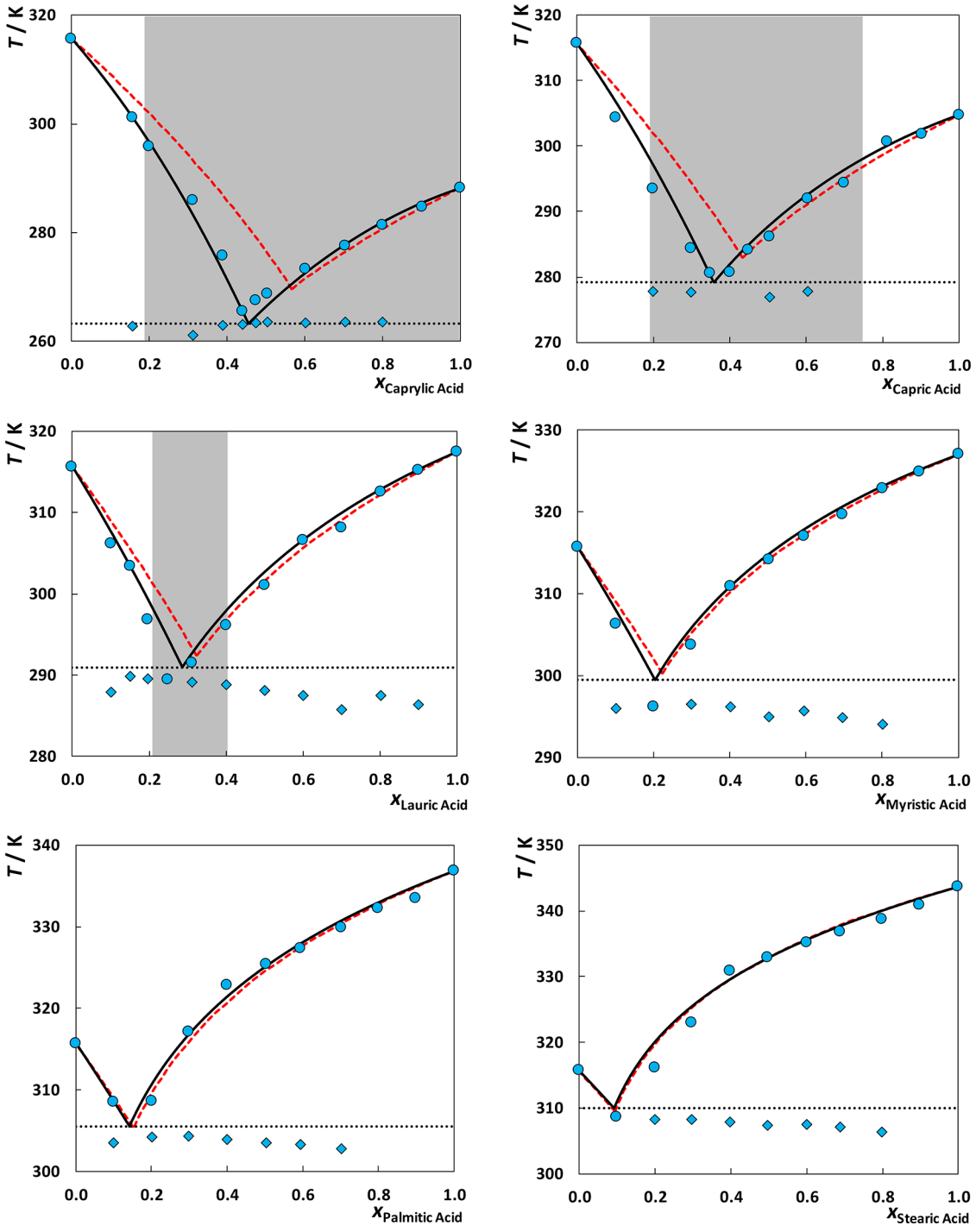

Figure 1. Solid−liquid phase diagrams of mixtures composed of monocarboxylic acids and L(−)-menthol. Symbols represent experimental data measured in this work, while lines represent the modeling results: red dashed line, Ideal; black solid line, PC-SAFT; black dotted line, T^E predicted by PC-SAFT. Gray regions represent the concentration range for which the mixture is liquid at room temperature (T = 298.15 K).

where γ_i^l is the activity coefficient of compound i in the liquid phase at a certain mole fraction composition x_i, T is the absolute temperature, T_m and $\Delta_{fus}H$ are the melting temperature and enthalpy of the pure solute, respectively, R is the universal gas constant, and $\Delta_m C_p$ is the difference between the heat capacity of compound i in the liquid and the solid states. Usually, the last term of eq 1 has a negligible value when compared with the first, especially for small differences between T and T_m, and thus, it was not taken into account in this work.[30,31]

If an ideal liquid phase is assumed, the activity coefficients are equal to unity (γ_i^l = 1), and the solubility curves can be easily obtained from eq 1 as a function of the temperature and the melting properties of the pure compounds. On the other hand, considering a nonideal behavior, experimental activity coefficients can be obtained from eq 1 using the experimental data (solubility at given temperatures). The liquidus lines can, in this case, be obtained through eq 1 but with the activity coefficients calculated through an appropriate activity coefficient model or EoS. In this work, PC-SAFT was used to model the phase diagrams, where the activity coefficients are obtained as the ratio between the fugacity coefficient of the solute in the liquid mixture and that of the pure compounds, both obtained from the system's residual Helmholtz energy calculated within the framework of the EoS.

DOI: 10.1021/acssuschemeng.8b01203
ACS Sustainable Chem. Eng. XXXX, XXX, XXX−XXX

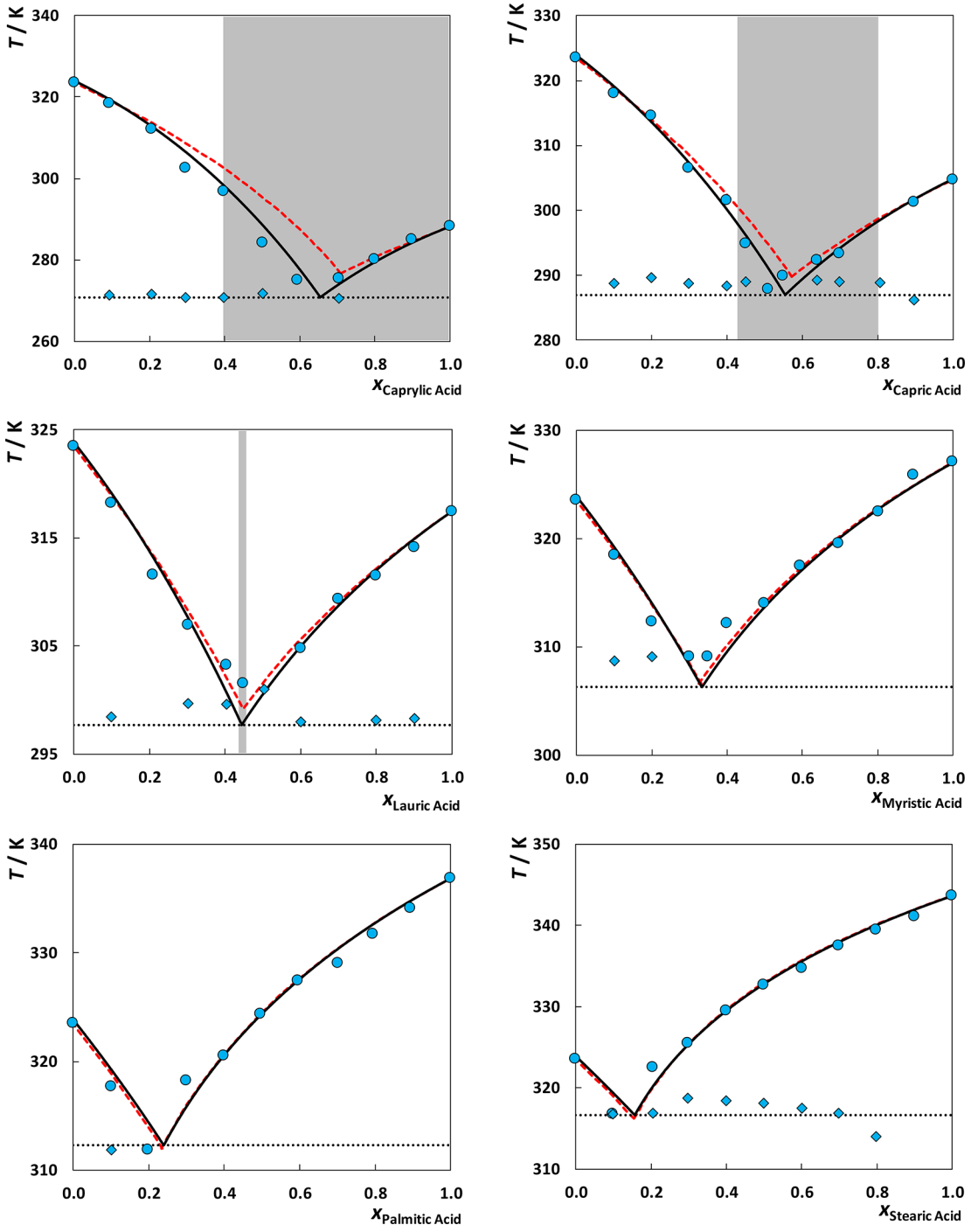

Figure 2. Solid–liquid phase diagrams of mixtures composed of monocarboxylic acids and thymol. Symbols represent experimental data measured in this work, while lines represent the modeling results: red dashed line, Ideal; black solid line, PC-SAFT; black dotted line, T^E predicted by PC-SAFT. Gray regions represent the concentration range for which the mixture is liquid at room temperature (T = 298.15 K).

PC-SAFT EoS. Because of the increasing complexity of the systems of interest in the chemical industry, there is a demand for broader and accurate thermodynamic models. Although cubic EoS's are still the standard and proven methods for many applications,[32] they have known limitations when modeling the thermodynamic behavior and phase equilibria of complex systems like DES that might present strong and short-range hydrogen-bonding interactions between their constituents. So far, molecular-based EoSs with a strong theoretical background derived from statistical mechanics emerge as one of the most promising alternatives to tackle these challenges.[23,33−35] These molecular-based EoSs can explicitly account for different structural and energetic effects on the thermodynamic properties and phase equilibria of a system. The foremost application of such a concept is the Statistical Associating Fluid Theory (SAFT) proposed by Chapman and co-workers in the late 1980s[36−39] based on Wertheim's first order thermodynamic perturbation theory,[40−43] where a hard-sphere reference fluid is perturbed by distinct contributions, reckoning particular effects such as the molecular shape, dispersive interactions, and hydrogen-bonding phenomenon. In the framework of SAFT, molecules were viewed as associating chains consisting of equally sized spherical segments bonded tangentially that may contain short-range associative sites.

Following the work of Chapman and co-workers, several SAFT-type equations have been proposed over the years mostly differing in the

DOI: 10.1021/acssuschemeng.8b01203
ACS Sustainable Chem. Eng. XXXX, XXX, XXX−XXX

chosen reference term. One of the most fruitful modifications is PC-SAFT,[20] which considers a hard chain of freely jointed hard spheres as a reference fluid (instead of a hard sphere). In the original publications,[20,44] PC-SAFT was demonstrated to perform better than the original model in several cases, especially for long-chain molecules. Moreover, it has already been successfully applied to eutectic mixtures.[23,34,45,46] The model equations are available in the SI as well as the detailed procedure applied to obtain the PC-SAFT pure component parameters.

RESULTS AND DISCUSSION

Solid−Liquid Phase Diagrams. The solid−liquid phase diagrams measured for the mixtures studied in this work are illustrated in Figures 1 and 2 and Figure S3, while the detailed data are listed in Tables S1 and S2 of the Supporting Information. These systems exhibit a phase behavior characterized by a single eutectic point, and although the melting point depressions are relatively small and close to those predicted assuming an ideal liquid phase, in many cases it allows the formation of liquid mixtures at room temperature, while both pure compounds are solid.

The SLE phase diagrams were described using two methodologies: (i) assuming an ideal liquid phase ($\gamma_i = 1$) and (ii) calculating the activity coefficients through the associative PC-SAFT EoS. The modeling results are displayed in Figures 1 and 2 along with the experimental data. Moreover, the activity coefficients of each compound in the liquid phase obtained from PC-SAFT are displayed in Figures S4 and S5 of the SI, and their experimental values (accessed from the solubility data through eq 1) reported in Tables S1 and S2.

The quasi-ideal behavior observed for these mixtures suggests that the hydrogen-bonding (HB) networks established in these mixtures are not significantly different in intensity to those present in the pure compounds.[23,47] Even if the systems under study are quasi-ideal, the terpene solubility curves show small negative deviations from the ideal behavior, decreasing with the acid's chain length increase. While for caprylic and capric acids the eutectic temperature deviates approximately 10 K from ideal behavior, for stearic acid these are essentially identical. These deviations from ideality suggest that the existence of interactions between the terpene and the short chain acid are slightly stronger than those observed in the pure terpenes. The decrease in the nonideality with the acid's chain length is probably due to an increase in the dispersive interactions that eventually become dominant on these systems with very long alkyl chains.

Figures 1 and 2 show that PC-SAFT can adequately correlate the SLE experimental data of mixtures involving thymol or L(−)-menthol and monocarboxylic acids. For the systems containing thymol, the PC-SAFT predictions using solely the pure-component parameters fitted to the pure liquid densities and vapor pressures were found to provide a very good description of the experimental data. On the other hand, for the systems with L(−)-menthol, a binary interaction parameter increasing the cross-association interactions between L(−)-menthol and the acids was required. These binary interaction parameters, listed in Table S3, were obtained through the minimization of the temperature (T) average absolute deviation (AAD/K) expressed as

$$\mathrm{AAD}/K = \frac{1}{N}\sum_{i=1}^{N} |T_i^{\mathrm{calc}}(K) - T_i^{\mathrm{exp}}(K)| \quad (2)$$

where T_i^{calc} and T_i^{exp} are the calculated and the experimental melting temperatures, respectively. The need for a binary interaction parameter to accurately describe quasi-ideal systems may seem surprising, but it might be related to an asymmetry present in these systems. It can be observed that the acid solubility curve displays an almost ideal behavior or presents slight positive deviations from ideality, conversely to what is observed in the terpene solubility curves. These unsymmetrical small deviations from ideality are difficult to be captured by most thermodynamic models, as discussed in our previous work.[34] Still, the low magnitude of the deviations from ideality allowed us to correlate the binary interaction parameter between L(−)-menthol and the carboxylic acids, with the molecular weight of the acid

$$k_{ij\_\mathrm{eps}} = 0.0004837 \times M_w(\mathrm{g/mol}) - 0.1336,\ R^2 = 0.9586 \quad (3)$$

As can be seen from eq 3, the absolute values of k_{ij_eps} estimated in the mixtures with L(−)-menthol decrease with an increase of the acid's chain length as previously observed in eutectic mixtures composed of $[N_{XXXX}]Cl$ + monocarboxylic acids.[23]

The average absolute deviations assuming ideality or using PC-SAFT are reported in Table S3. PC-SAFT EoS decreases the AAD relatively to the ideality results for most systems, especially in those exhibiting negative deviations from the ideal behavior in the terpene solubility curve. This stresses the advantage of using EoSs able to explicitly account for hydrogen-bonding interactions and emphasizes the usefulness of PC-SAFT to describe the thermodynamic behavior of eutectic mixtures and DES.

Since PC-SAFT was able to accurately describe the experimental solubility curves of mixtures of terpenes and monocarboxylic acids, it was used to provide estimates of their eutectic points. These are shown in Figure 3 and detailed in Table S4.

As depicted in Figure 3, in some cases the eutectic composition predicted by PC-SAFT is somewhat different from that predicted assuming ideality. This difference is smaller for mixtures with thymol than for mixtures with L(−)-menthol. For both sets (thymol + monocarboxylic acids and L(−)-menthol + monocarboxylic acids) of phase diagrams, the eutectic temperature was observed to regularly increase with the acids molecular weight, as shown in Figure 3 and Figure S3. The mole fraction of carboxylic acid at the eutectic composition, oppositely, decreases with increasing acid molecular weight. Moreover, a fixed stoichiometric relationship between the hydrogen bond donor and acceptor cannot be observed. Instead, a continuous change with the acid chain length can be observed in Figure 3, stressing the highly tunable character of the eutectic point of these mixtures and the wide concentration range to formulate these eutectic solvents as highlighted in Figures 1 and 2.

In Figure S6, the SLE behavior of lauric acid with the terpenes (L(−)-menthol and thymol) is depicted. The results show that the change in the terpene used has no influence on the qualitative behavior of the acid's solubility curve. However, the different melting properties of thymol and L(−)-menthol, and the possibility of cross-association with acid molecules, are found to considerably influence the terpene solubility curve resulting in different eutectic points, both in temperature and composition, as correctly described by the PC-SAFT EoS.

DOI: 10.1021/acssuschemeng.8b01203
ACS Sustainable Chem. Eng. XXXX, XXX, XXX−XXX

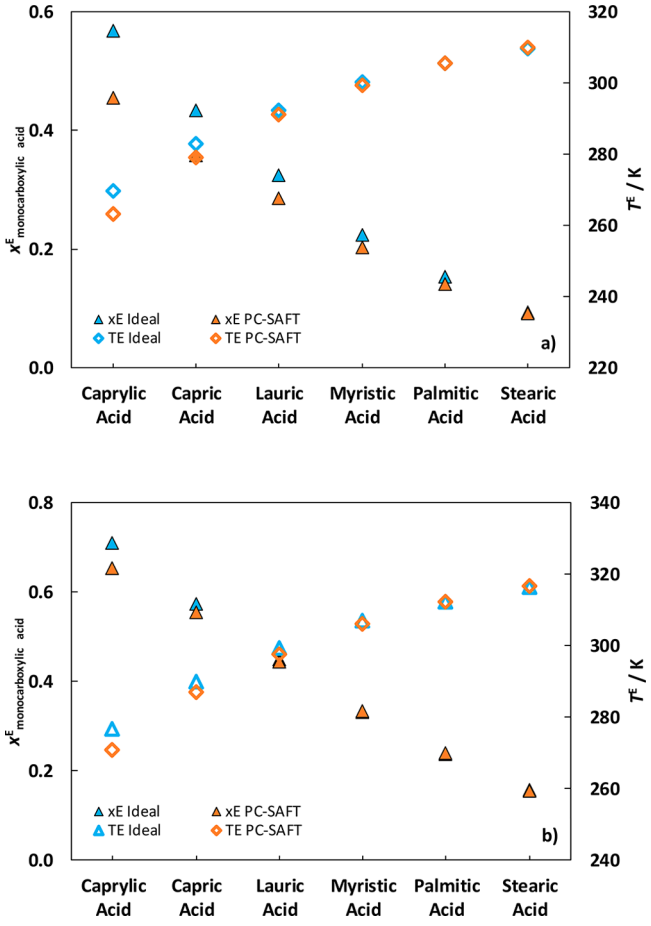

Figure 3. Eutectic compositions and temperatures of the systems involving (a) L(−)-menthol and (b) thymol.

For comparison purposes, little information has been found that also supports the importance of modeling tasks. Ribeiro et al.[17] reported 286.99 K as the melting point of the mixture DL-menthol and lauric acid at 0.66:0.33 (mole fraction ratio). In this work, the values measured (at nearby compositions) were 291.54 K at the composition ratio 0.69:0.31 and 296.17 K at the composition ratio 0.60:0.40. The value predicted using PC-SAFT EoS at the exact composition ratio 0.66:0.33 is 293.97 K. Moreover, the eutectic temperature predicted by PC-SAFT was 290.97 K at 0.71:0.29.

In order to evaluate the systems involving thymol + monocarboxylic acid and L(−)-menthol + monocarboxylic acid as potential solvents, their mixtures with compositions close to the eutectic point are characterized in the next sections. Density and viscosity are relevant solvent properties since they have an important impact on mass transport phenomena affecting solvents suitability for specific applications, while the solvatochromic parameters help to define the mixtures polarity aiming at better understand the influence of the components chemical structure on their properties for a priori design of eutectic mixtures.

Densities. Densities of the eutectic mixtures were determined at atmospheric pressure in the temperature range between 278.15 and 373.15 K and are reported in Figure S7 and Tables S5 and S6 of the SI, along with the mole fraction of the monocarboxylic acid. The densities of pure thymol and L(−)-menthol[48] are also displayed in Figure S7 for comparative purposes.

While all mixtures studied are less dense than water, eutectic mixtures with thymol present higher densities than those with L(−)-menthol, and their range of variation is also broader. The densities of the eutectic mixtures of monocarboxylic acids with L(−)-menthol decrease with increasing alkyl chain of the monocarboxylic acid. Concerning the mixtures with thymol, the opposite trend is observed, i.e., the densities decrease with decreasing chain length of the monocarboxylic acid. This is explained by the fact that the density of pure thymol is higher than the correspondent mixtures with the monocarboxylic acids, while the density of pure L(−)-menthol is in between those with the acids (Figure S7). Thus, and taking into account that at the eutectic point when increasing the alkyl chain length of the fatty acid the molar fraction of terpene increases, by adding thymol, the mixtures densities tend to increase, while adding L(−)-menthol densities have a tendency to decrease.

Since the SLE of the different systems analyzed was successfully described using the PC-SAFT EoS, the ability of this model to predict the densities of these systems was also investigated. The results are presented in Figure S7, and the AAD to the experimental densities are presented in Table S7. The deviations obtained range between 0.02% and 1.35% with an average value (for all 183 data points) of 0.46%.

The excess molar volumes, V_m^E, were calculated[49] through the experimental density data measured in this work (Tables S5 and S6) and are depicted in Figure S8. The densities of pure thymol, L(−)-menthol, and monocarboxylic acids were taken from the literature.[48,50,51] Here, V_m^E are, in general, close to zero, reinforcing the ideal character of these mixtures. Mixtures involving L(−)-menthol present mainly negative excess molar volumes, while the opposite is observed for thymol. Almost no dependence with temperature is observed. Since the excess molar volumes are negligible, the molar volume of the mixture can be directly calculated through the densities of the pure components.[52] The average absolute deviations are 0.21 and 0.27 $cm^3 \cdot mol^{-1}$ for mixtures involving L(−)-menthol and thymol, respectively.

Additionally, a study on the isobaric thermal expansion coefficients, α_p, was performed and is presented in SI. The derived α_p values are, in general, very similar, varying between -8.5×10^{-4} and -8.9×10^{-4}. No well-defined dependence of α_p with the chain length of the monocarboxylic acid was observed within the uncertainty of the experimental data. Moreover, the α_p of eutectic mixtures containing either caprylic, palmitic, or stearic acids varies significantly with the selected terpene. With the exception of caprylic acid, the isobaric thermal expansion coefficients are higher in the eutectic mixtures with thymol than in those containing L(−)-menthol. Regarding the α_p values predicted using PC-SAFT, they increase with the chain length of the monocarboxylic acid. Moreover, no significant difference is observed when using thymol or L(−)-menthol. Experimental and calculated α_p values present significant differences in mixtures involving the caprylic and capric acids, but they also suggest that the α_p values decrease for the eutectic mixtures of acids above myristic.

Viscosities. Viscosity data for the eutectic mixtures under study were also measured at atmospheric pressure in the temperature range between 278.15 and 373.15 K, which are depicted in Figure S9 and detailed in Tables S8 and S9. For comparative purposes, the viscosities of pure thymol and L(−)-menthol were also measured and are shown in Figure S9 and Tables S8 and S9.

DOI: 10.1021/acssuschemeng.8b01203
ACS Sustainable Chem. Eng. XXXX, XXX, XXX−XXX

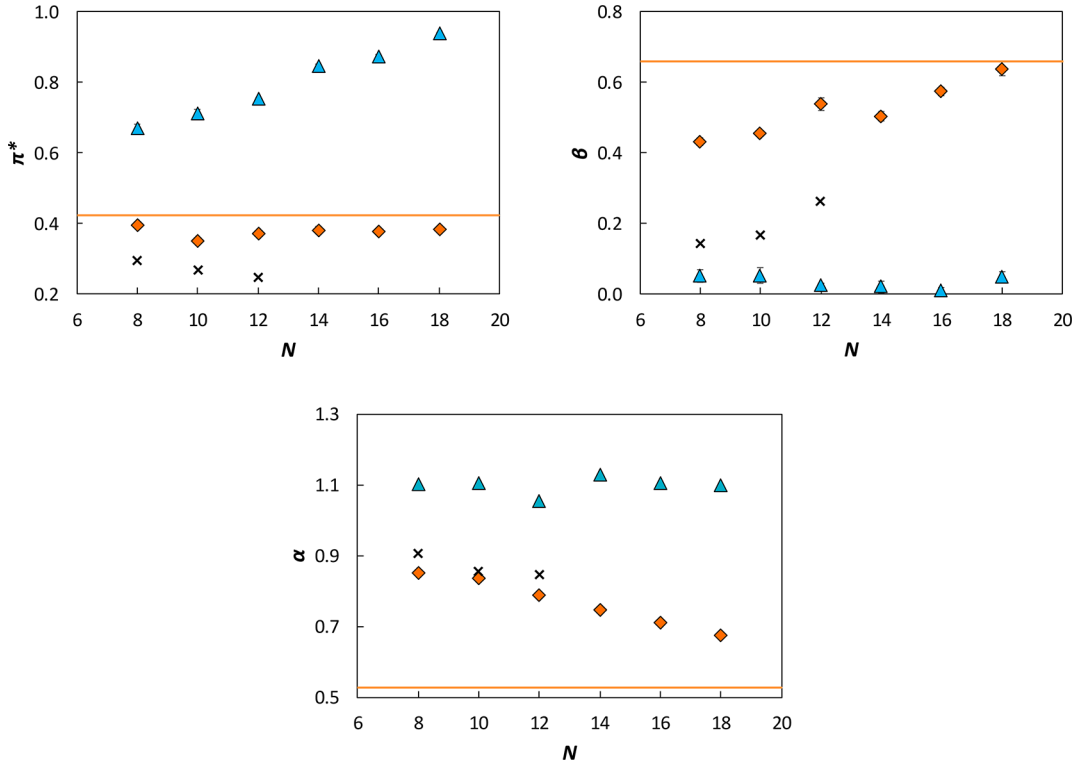

Figure 4. Kamlet−Taft solvatochromic parameters of the different pure compounds and mixtures studied at 323.15 K, as a function of the number of carbons of the monocarboxylic acid, *N*. Legend: blue triangle, thymol + monocarboxylic acid; orange diamond, L(−)-menthol + monocarboxylic acid; orange solid line, pure L(−)-menthol; black crosses, pure monocarboxylic acids.

The viscosity values are fairly low for this type of solvent and are observed to increase with acid chain length. However, the effect of chain length is much less relevant at higher temperatures where viscosity values are very similar. Contrary to what is observed for the densities, the range of viscosities of eutectic mixtures of L(−)-menthol is broader than the range of viscosities of eutectic mixtures involving thymol, and thymol-based eutectic mixtures are significantly less viscous.

A comparison between the viscosity of pure compounds and their mixtures is displayed in Figure S10. The viscosities of pure monocarboxylic acids were taken from the literature.[50,51] In most cases, the viscosity of the mixtures is in between (or higher) the viscosities of the pure components. There are only two conditions where the viscosity of the mixture is lower than the viscosity of both pure components: L(−)-menthol + lauric acid at 333.15 K and L(−)-menthol + myristic acid at 328.15 K. For caprylic and capric acids, their pure viscosities are generally lower than the viscosities of their mixtures with terpenes. For heavier acids, viscosities of the pure compounds are higher than those for mixtures with terpenes. Regarding L(−)-menthol, the viscosity of pure terpene is higher than the viscosity of the mixture involving monocarboxylic acids with chains lengths from C8 to C14, when the viscosity of pure terpene becomes lower. The viscosity of pure thymol is only higher in the system involving caprylic acid. Additionally, the viscosity ideal mixture rule[49] ($\ln \eta_{mix} = x_1 \ln \eta_1 + x_2 \ln \eta_2$) was applied and proved to correctly describe the experimental data. The average absolute deviation between the predicted (by the viscosity ideal mixture rule) and the experimental was of 0.19 and 0.28 mPa·s for mixtures involving L(−)-menthol and thymol, respectively.

The energy barrier (E), i.e., the energy value that must be overcome in order for the molecules to move past each other[53] was also investigated (study available in the SI). Here, E is observed to be lower for the thymol eutectic mixtures and to increase with the chain length of the monocarboxylic acid used in the mixture. The addition of monocarboxylic acids decreases the energy barrier, with this decrease being more pronounced when using thymol and small monocarboxylic acids.

Kamlet−Taft Solvatochromic Parameters. The Kamlet−Taft parameters were measured at 323.15 K and are presented in Figure 4 and Table S10 (equations available in the SI). The solvatochromic π^* is related with the polarizability/dipolarity of the mixture. This is higher for mixtures involving thymol due to the presence of the aromatic ring in the structure. Although it is not available for pure thymol due to its higher melting point, it is expected to be larger than for L(−)-menthol. Moreover, there is an almost linear increase with the number of carbons of the alkyl chain length of the monocarboxylic acid, which is probably connected to the simultaneous increase in the thymol mole fraction at the eutectic point. The π^* for the L(−)-menthol-based eutectic solvents does not vary with the acid used, presenting an almost constant value, close to the value of pure L(−)-menthol.

The β and α parameters describe the hydrogen bond acceptor and donor capacity, respectively. The variation observed on parameter β are the opposite of those discussed for parameter π^*: L(−)-menthol presents higher values than thymol and increases linearly with the number of carbons of the monocarboxylic acid, while for mixtures with thymol this value is practically constant and very close to zero. This is related to the aromatic nature of the ring on thymol that substantially reduced its ability to act as a hydrogen bonding acceptor. The capacity to act as a hydrogen bond donor is higher in mixtures with thymol, being almost independent of the alkyl chain length

DOI: 10.1021/acssuschemeng.8b01203
ACS Sustainable Chem. Eng. XXXX, XXX, XXX−XXX

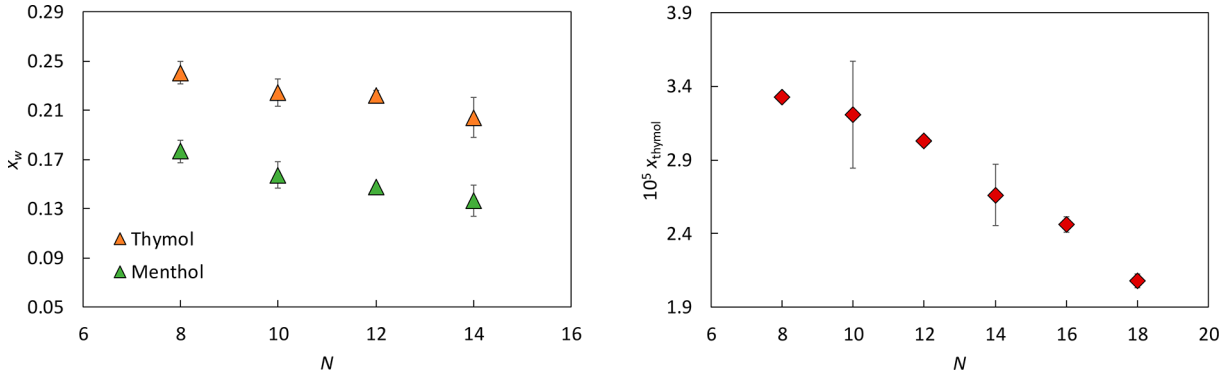

Figure 5. Solubility of water in the eutectic mixtures, x_w, and solubility of thymol (+ monocarboxylic acids), x_{thymol}, in water at 298.15 K and as a function of the number of carbons of the alkyl chain length of the monocarboxylic acid, *N*.

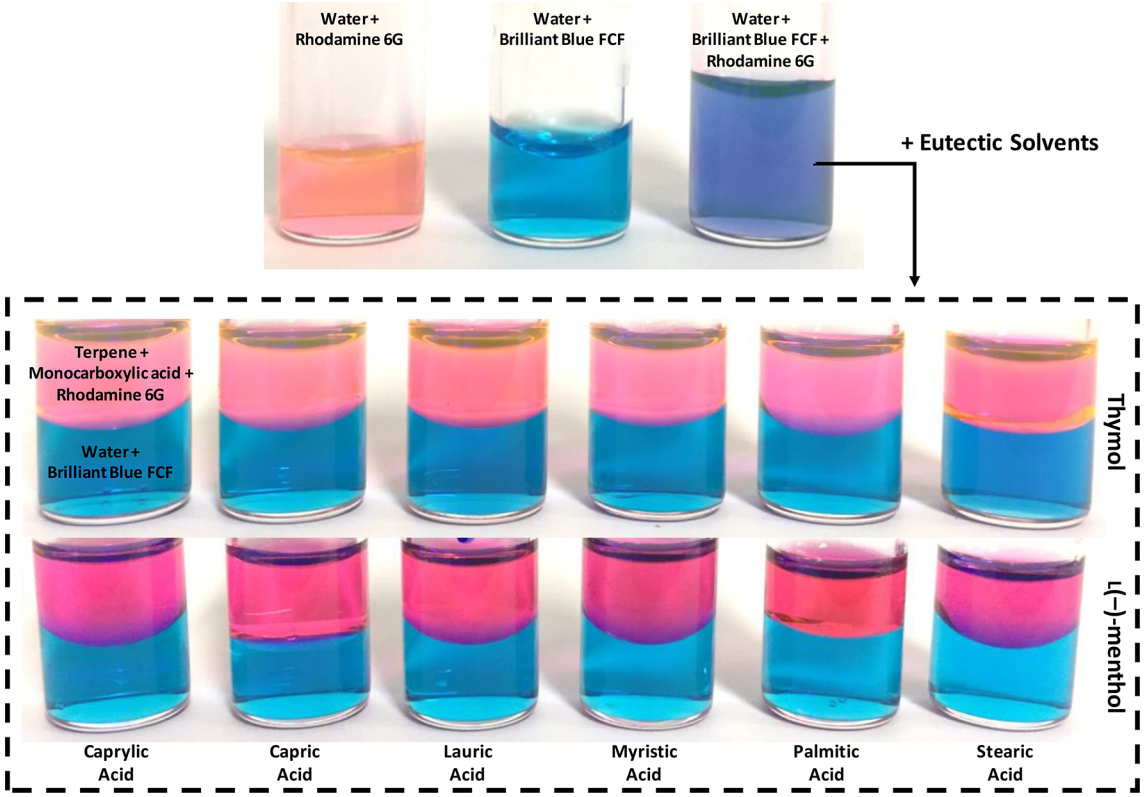

Figure 6. Mixture of the solvents investigated in this work with water and the dyes Rhodamine 6G and Brilliant Blue FCF.

of the acid, while in mixtures containing L(−)-menthol α decreases linearly with the number of carbons of the alkyl chain of the acid, on a trend that evolves toward the value of the pure L(−)-menthol.

In order to evaluate the consistency of these results, the sigma profiles of thymol and L(−)-menthol were computed by COSMO-RS and are presented in Figure S11. These profiles suggest that L(−)-menthol has a larger capacity to accept hydrogen bonds and thus should have a higher β, while thymol has a bigger capacity to donate H-bonds, and thus should present a higher α. Moreover, the addition of nonpolar groups to the monocarboxylic acid that do not have the capacity to form hydrogen bonding leads to the decrease in α and increase in β, as observed for L(−)-menthol.

Florindo et al.[54] measured the Kamlet−Taft solvatochromic parameters of mixtures of L(−)-menthol with caprylic (β = 0.43/0.50, π^* = 0.39/0.41, α = 0.85/1.77) and lauric (β = 0.54/0.57, π^* = 0.37/0.37, α = 0.79/1.79) acids. The only parameter that presents significant differences between the two sets of experimental data is the hydrogen-bond donor acidity, α. This was obtained using different probes and different methodologies that can be the reason for the differences observed, once the solvatochromic parameters are probe dependent.

To evaluate the potential of these mixtures as solvents, comparisons with other molecular solvents are discussed. The Kamlet−Taft solvatochromic parameters of some common solvents are displayed in Table S10. In general, mixtures involving thymol display a higher ability to establish nonspecific interactions with a solute than organic solvents, as supported by the higher value of π^*. On the other hand, these thymol-based mixtures present higher hydrogen-bond acidity values than alcohols, ketones, alkanes, aromatics, and the pure acids and slightly lower values than water. Regarding the ability to accept protons, mixtures involving L(−)-menthol present similar

DOI: 10.1021/acssuschemeng.8b01203
ACS Sustainable Chem. Eng. XXXX, XXX, XXX−XXX

values to water and other organic solvents, while the mixtures involving thymol present values close to zero like hydrocarbons, meaning no ability to accept protons.

To assess the hydrophobicity of the studied systems, quantitative studies on the mutual solubilities of the investigated mixtures (with compositions close to the eutectic point; Tables S5 and S6) with water were performed at 298.15 K, and the results are presented in Figure 5 and Table S11. The solubility of the L(−)-menthol in water was not measured since this compound was not possible to quantify using the analytical technique adopted. As shown in Figure 5, the solubility of water in the eutectic mixtures decreases with the increase in the alkyl chain length of the acid, i.e., the hydrophobicity of the HBD. The same trend is observed for the solubility of thymol (+ monocarboxylic acids) in water. When comparing with the solubility of pure thymol in water at 298.15 K ($x_{thymol} = 11.8 \times 10^{-5}$),[8] it is possible to conclude that the presence of the acid in the mixture decreases the solubility of terpene in more than 1 order of magnitude. The solubilities of the pure acids in water vary from $x_{caprylic\ acid} = 9.88 \times 10^{-5}$ ($T = 303.15$ K) to $x_{stearic\ acid} = 3.79 \times 10^{-8}$ ($T = 298.15$ K).[55]

Additionally, the systems investigated were mixed with water (in exactly the same masses of 500 μL each) in the presence of dyes. Results are presented in Figure 6 that shows a separation between the organic and aqueous phases. Rhodamine 6G, presenting a nonpolar character, seems to be completely extracted into the hydrophobic organic phase (pink-dyed phase), terpene + monocarboxylic acid. On the other hand, the Brilliant Blue FCF (E133) migrates into the water phase (blue-dyed phase).

In summary, we investigated mixtures involving terpenes and monocarboxylic acids aiming to characterize and design these solvents. The SLE phase diagrams of the mixtures were measured in the whole composition range using DSC and showed a broader composition range in the liquid state at room temperature than previously admitted. Generally, the systems exhibited small deviations from ideality and a eutectic point close to that predicted assuming ideality. Therefore, although often labeled as DES, these systems do not present negative deviations large enough to induce a significant melting point depression. However, it must be stressed that room temperature solvents can be obtained for many of these mixtures on a wide composition range and not fixed to any particular stoichiometric relationship between the hydrogen bond donor and acceptor, even at the eutectic point, which reinforces the tunable character of the liquid phase region of these mixtures. The experimental solid−liquid phase diagrams were successfully described using the PC-SAFT EoS, which provided reliable estimates of the eutectic points and of the solvents densities. This EoS also showed that liquid phases are quasi-ideal. The eutectic mixtures present densities lower than water and low viscosities (1.3−50.6 mPa·s), and in general, eutectic mixtures containing thymol were less viscous but more dense than those with L(−)-menthol. A series of solvatochromic parameters were measured in order to address the polarity of the mixtures investigated. All the parameters are strongly influenced by the terpene used and in some cases vary with the alkyl chain length of the monocarboxylic acid. Mixtures involving thymol present a higher hydrogen-bond acidity character, as well as higher nonspecific interactions. L(−)-Menthol presents a higher hydrogen-bond basicity character and a slight increase in this parameter with the increase in the alkyl chain of the monocarboxylic acid. Moreover, the mixtures reported here display a high capacity to donate (thymol-based mixtures) and accept (L(−)-menthol-based mixtures) protons when compared to some organic molecular solvents and very close to water. The polarity dependence on the alkyl chain length of the monocarboxylic acid favors the design of new solvents. The measured mutual solubilities with water prove the hydrophobic character of the mixtures investigated.

■ ASSOCIATED CONTENT

Supporting Information

The Supporting Information is available free of charge on the ACS Publications website at DOI: 10.1021/acssuschemeng.8b01203.

Structures of the investigated compounds; mixtures NMR; experimental and calculated solid−liquid phase diagrams and activity coefficients; densities, excess molar volumes, and isobaric thermal expansion coefficients; viscosities and energy barrier; Kamlet−Taft solvatochromic parameters; sigma profiles of pure compounds; mutual solubilities with water; PC-SAFT parameters, their description, and calculation; ideal and predicted (PC-SAFT) eutectic points; densities, viscosities, and KT solvatochromic parameters equations. (PDF)

■ AUTHOR INFORMATION

Corresponding Author

*E-mail: jcoutinho@ua.pt. Phone: +351 234401507. Fax: + 351 234370084.

ORCID

Mónia A. R. Martins: 0000-0003-0748-1612
Emanuel A. Crespo: 0000-0003-2137-0564
Christoph Held: 0000-0003-1074-177X
Simão P. Pinho: 0000-0002-9211-857X
João A. P. Coutinho: 0000-0002-3841-743X

Notes

The authors declare no competing financial interest.

■ ACKNOWLEDGMENTS

This work was developed in the scope of the project CICECO − Aveiro Institute of Materials, POCI-01-0145-FEDER-007679 (ref. FCT UID/CTM/50011/2013) and Associate Laboratory LSRE-LCM, POCI-01-0145-FEDER-006984 (ref. FCT UID/EQU/50020/2013), both financed by national funds through the FCT/MEC and when appropriate cofinanced by FEDER under the PT2020 Partnership Agreement. This work is also a result of project "AIProcMat@N2020 − Advanced Industrial Processes and Materials for a Sustainable Northern Region of Portugal 2020", with the reference NORTE-01-0145-FEDER-000006, supported by Norte Portugal Regional Operational Programme (NORTE 2020), under the Portugal 2020 Partnership Agreement, through the European Regional Development Fund (ERDF). M.A.R.M acknowledges FCT for her Ph.D. grant (SFRH/BD/87084/2012). FCT is also acknowledged for funding the project DeepBiorefinery (PTDC/AGRTEC/1191/2014). P.V.A.P. and G.J.M. thank the national funding agencies CNPq (National Council for Scientific and Technological Development) (305870/2014-9, 309780/2014-4, 140702/2017-2, 406918/2016-3, 406963/2016-9), FAPESP (Research Support Foundation of the State of Sao Paulo) (2014/21252-0, 2016/08566-1), FAEPEX/UNICAMP (Fund for Research, Teaching, and Extension)

DOI: 10.1021/acssuschemeng.8b01203
ACS Sustainable Chem. Eng. XXXX, XXX, XXX−XXX

(0125/16), and CAPES (Coordination of Improvement of Higher Level Personnel) for financial support and scholarships. E.A.C thanks FCT for the Ph.D. grant SFRH/BD/130870/2017. C.H. acknowledges financial support from Max – Buchner Research Foundation and from German Science Foundation (DFG) HE 7165/7-1.

REFERENCES

(1) Zhang, Q.; De Oliveira Vigier, K.; Royer, S.; Jérôme, F. Deep Eutectic Solvents: Syntheses, Properties and Applications. *Chem. Soc. Rev.* **2012**, *41* (21), 7108−7146.

(2) Florindo, C.; Oliveira, F. S.; Rebelo, L. P. N.; Fernandes, A. M.; Marrucho, I. M. Insights into the Synthesis and Properties of Deep Eutectic Solvents Based on Cholinium Chloride and Carboxylic Acids. *ACS Sustainable Chem. Eng.* **2014**, *2* (10), 2416−2425.

(3) Maugeri, Z.; Domínguez de María, P. Novel Choline-Chloride-Based Deep-Eutectic-Solvents with Renewable Hydrogen Bond Donors: Levulinic Acid and Sugar-Based Polyols. *RSC Adv.* **2012**, *2* (2), 421−425.

(4) van Osch, D. J. G. P.; Zubeir, L. F.; van den Bruinhorst, A.; Rocha, M. A. A.; Kroon, M. C. Hydrophobic Deep Eutectic Solvents as Water-Immiscible Extractants. *Green Chem.* **2015**, *17* (9), 4518−4521.

(5) Florindo, C.; Branco, L. C.; Marrucho, I. M. Development of Hydrophobic Deep Eutectic Solvents for Extraction of Pesticides from Aqueous Environments. *Fluid Phase Equilib.* **2017**, *448* (25), 135−142.

(6) van Osch, D. J. G. P.; Parmentier, D.; Dietz, C. H. J. T.; van den Bruinhorst, A.; Tuinier, R.; Kroon, M. C. Removal of Alkali and Transition Metal Ions from Water with Hydrophobic Deep Eutectic Solvents. *Chem. Commun.* **2016**, *52* (80), 11987−11990.

(7) Tereshatov, E. E.; Boltoeva, M. Y.; Folden, C. M. First Evidence of Metal Transfer into Hydrophobic Deep Eutectic and Low-Transition-Temperature Mixtures: Indium Extraction from Hydrochloric and Oxalic Acids. *Green Chem.* **2016**, *18* (17), 4616−4622.

(8) Martins, M. A. R.; Silva, L. P.; Ferreira, O.; Schröder, B.; Coutinho, J. A. P.; Pinho, S. P. Terpenes Solubility in Water and Their Environmental Distribution. *J. Mol. Liq.* **2017**, *241*, 996−1002.

(9) Shen, Q.; Li, X.; Li, W.; Zhao, X. Enhanced Intestinal Absorption of Daidzein by Borneol/Menthol Eutectic Mixture and Microemulsion. *AAPS PharmSciTech* **2011**, *12* (4), 1044−1049.

(10) Phaechamud, T.; Tuntarawongsa, S. Transformation of Eutectic Emulsion to Nanosuspension Fabricating with Solvent Evaporation and Ultrasonication Technique. *Int. J. Nanomed.* **2016**, *11*, 2855−2865.

(11) Mohammadi-Samani, S.; Yousefi, G.; Mohammadi, F.; Ahmadi, F. Meloxicam Transdermal Delivery: Effect of Eutectic Point on the Rate and Extent of Skin Permeation. *Iran. J. Basic Med. Sci.* **2014**, *17* (2), 112−118.

(12) Stott, P. W.; Williams, A. C.; Barry, B. W. Transdermal Delivery from Eutectic Systems: Enhanced Permeation of a Model Drug. *J. Controlled Release* **1998**, *50* (1−3), 297−308.

(13) Yong, C. S.; Jung, S. H.; Rhee, J.-D.; Choi, H.-G.; Lee, B.-J.; Kim, D.-C.; Choi, Y. W.; Kim, C.-K. Improved Solubility and In Vitro Dissolution of Ibuprofen from Poloxamer Gel Using Eutectic Mixture with Menthol. *Drug Delivery* **2003**, *10* (3), 179−183.

(14) Kaplun-Frischoff, Y.; Touitou, E. Testosterone Skin Permeation Enhancement by Menthol through Formation of Eutectic with Drug and Interaction with Skin Lipids. *J. Pharm. Sci.* **1997**, *86* (12), 1394−1399.

(15) Kang, L.; Jun, H. W.; McCall, J. W. Physicochemical Studies of Lidocaine-Menthol Binary Systems for Enhanced Membrane Transport. *Int. J. Pharm.* **2000**, *206* (1−2), 35−42.

(16) Nazzal, S.; Smalyukh, I.; Lavrentovich, O.; Khan, M. A. Preparation and in Vitro Characterization of a Eutectic Based Semisolid Self-Nanoemulsified Drug Delivery System (SNEDDS) of Ubiquinone: Mechanism and Progress of Emulsion Formation. *Int. J. Pharm.* **2002**, *235* (1), 247−265.

(17) Ribeiro, B. D.; Florindo, C.; Iff, L. C.; Coelho, M. A. Z.; Marrucho, I. M. Menthol-Based Eutectic Mixtures: Hydrophobic Low Viscosity Solvents. *ACS Sustainable Chem. Eng.* **2015**, *3* (10), 2469−2477.

(18) Aroso, I. M.; Craveiro, R.; Rocha, Â.; Dionísio, M.; Barreiros, S.; Reis, R. L.; Paiva, A.; Duarte, A. R. C. Design of Controlled Release Systems for THEDES—Therapeutic Deep Eutectic Solvents, Using Supercritical Fluid Technology. *Int. J. Pharm.* **2015**, *492* (1), 73−79.

(19) Aroso, I. M.; Silva, J. C.; Mano, F.; Ferreira, A. S. D.; Dionísio, M.; Sá-Nogueira, I.; Barreiros, S.; Reis, R. L.; Paiva, A.; Duarte, A. R. C. Dissolution Enhancement of Active Pharmaceutical Ingredients by Therapeutic Deep Eutectic Systems. *Eur. J. Pharm. Biopharm.* **2016**, *98*, 57−66.

(20) Gross, J.; Sadowski, G. Perturbed-Chain SAFT: An Equation of State Based on a Perturbation Theory for Chain Molecules. *Ind. Eng. Chem. Res.* **2001**, *40* (4), 1244−1260.

(21) Okuniewski, M.; Paduszyński, K.; Domańska, U. (Solid + Liquid) Equilibrium Phase Diagrams in Binary Mixtures Containing Terpenes: New Experimental Data and Analysis of Several Modelling Strategies with Modified UNIFAC (Dortmund) and PC-SAFT Equation of State. *Fluid Phase Equilib.* **2016**, *422*, 66−77.

(22) Domalski, E. S.; Hearing, E. D. Heat Capacities and Entropies of Organic Compounds in the Condensed Phase. *J. Phys. Chem. Ref. Data* **1996**, *25* (1), 1−525.

(23) Pontes, P. V. A.; Crespo, E. A.; Martins, M. A. R.; Silva, L. P.; Neves, C. M. S. S.; Maximo, G. J.; Hubinger, M. D.; Batista, E. A. C.; Pinho, S. P.; Coutinho, J. A. P.; et al. Measurement and PC-SAFT Modeling of Solid-Liquid Equilibrium of Deep Eutectic Solvents of Quaternary Ammonium Chlorides and Carboxylic Acids. *Fluid Phase Equilib.* **2017**, *448*, 69−80.

(24) Misra, A. K.; Misra, M.; Panpalia, G. M.; Dorle, A. K. Thermoanalytical and Microscopic Investigation of Interaction between Paracetamol and Fatty Acid Crystals. *J. Macromol. Sci., Part A: Pure Appl.Chem.* **2007**, *44* (7), 685−690.

(25) Hong, J.; Hua, D.; Wang, X.; Wang, H.; Li, J. Solid-Liquid-Gas Equilibrium of the Ternaries Ibuprofen + Myristic Acid + CO2 and Ibuprofen + Tripalmitin + CO2. *J. Chem. Eng. Data* **2010**, *55* (1), 297−302.

(26) Schneider, H.; Badrieh, Y.; Migron, Y.; Marcus, Y. Hydrogen Bond Donation Properties of Organic Solvents and Their Aqueous Mixtures from 13 C NMR Data of Pyridine-n-Oxide. *Z. Phys. Chem.* **1992**, *177* (2), 143−156.

(27) Teles, A. R. R.; Capela, E. V.; Carmo, R. S.; Coutinho, J. A. P.; Silvestre, A. J. D.; Freire, M. G. Solvatochromic Parameters of Deep Eutectic Solvents Formed by Ammonium-Based Salts and Carboxylic Acids. *Fluid Phase Equilib.* **2017**, *448*, 15−21.

(28) Schröder, B.; Martins, M. A. R. R.; Coutinho, J. A. P. P.; Pinho, S. P. Aqueous Solubilities of Five N-(Diethylaminothiocarbonyl)-Benzimido Derivatives at T = 298.15 K. *Chemosphere* **2016**, *160*, 45−53.

(29) Prausnitz, J. M.; Lichtenthaler, R. N.; Azevedo, E. G. *Molecular Thermodynamics Fluid Phase Equilibria*; Prentice-Hall, 1986.

(30) Gmehling, J.; Kolbe, B.; Kleiber, M.; Rarey, J. *Chemical Thermodynamics for Process Simulation*; Wiley-VCH, 2012.

(31) Coutinho, J. A. P.; Andersen, S. I.; Stenby, E. H. Evaluation of Activity Coefficient Models in Prediction of Alkane Solid-Liquid Equilibria. *Fluid Phase Equilib.* **1995**, *103* (1), 23−39.

(32) Hendriks, E. M. Applied Thermodynamics in Industry, a Pragmatic Approach. *Fluid Phase Equilib.* **2011**, *311*, 83−92.

(33) Passos, H.; Khan, I.; Mutelet, F.; Oliveira, M. B.; Carvalho, P. J.; Santos, L. M. N. B. F.; Held, C.; Sadowski, G.; Freire, M. G.; Coutinho, J. A. P. Vapor-Liquid Equilibria of Water plus Alkylimidazolium-Based Ionic Liquids: Measurements and Perturbed-Chain Statistical Associating Fluid Theory Modeling. *Ind. Eng. Chem. Res.* **2014**, *53* (9), 3737−3748.

(34) Crespo, E. A.; Silva, L. P.; Martins, M. A. R.; Fernandez, L.; Ortega, J.; Ferreira, O.; Sadowski, G.; Held, C.; Pinho, S. P.; Coutinho, J. A. P. Characterization and Modeling of the Liquid Phase of Deep Eutectic Solvents Based on Fatty Acids/Alcohols and Choline Chloride. *Ind. Eng. Chem. Res.* **2017**, *56* (42), 12192−12202.

DOI: 10.1021/acssuschemeng.8b01203
ACS Sustainable Chem. Eng. XXXX, XXX, XXX−XXX

(35) Paduszyński, K.; Okuniewski, M.; Domańska, U. Sweet-in-Green" Systems Based on Sugars and Ionic Liquids: New Solubility Data and Thermodynamic Analysis. *Ind. Eng. Chem. Res.* **2013**, *52* (51), 18482−18491.
(36) Jackson, G.; Chapman, W. G.; Gubbins, K. E. Phase Equilibria of Associating Fluids of Spherical and Chain Molecules. *Int. J. Thermophys.* **1988**, *9* (5), 769−779.
(37) Chapman, W. G.; Jackson, G.; Gubbins, K. E. Phase Equilibria of Associating Fluids: Chain Molecules with Multiple Bonding Sites. *Mol. Phys.* **1988**, *65* (5), 1057−1079.
(38) Chapman, W. G.; Gubbins, K. E.; Jackson, G.; Radosz, M. SAFT: Equation-of-State Solution Model for Associating Fluids. *Fluid Phase Equilib.* **1989**, *52*, 31−38.
(39) Chapman, W. G.; Gubbins, K. E.; Jackson, G.; Radosz, M. New Reference Equation of State for Associating Liquids. *Ind. Eng. Chem. Res.* **1990**, *29* (8), 1709−1721.
(40) Wertheim, M. S. Fluids with Highly Directional Attractive Forces. *J. Stat. Phys.* **1984**, *35* (1), 19−34.
(41) Wertheim, M. S. Fluids with Highly Directional Attractive Forces. II. Thermodynamic Perturbation Theory and Integral Equations. *J. Stat. Phys.* **1984**, *35* (1), 35−47.
(42) Wertheim, M. S. Fluids with Highly Directional Attractive Forces. III. Multiple Attraction Sites. *J. Stat. Phys.* **1986**, *42* (3), 459−476.
(43) Wertheim, M. S. Fluids with Highly Directional Attractive Forces. IV. Equilibrium Polymerization. *J. Stat. Phys.* **1986**, *42* (3), 477−492.
(44) Gross, J.; Sadowski, G. Application of the Perturbed-Chain SAFT Equation of State to Associating Systems. *Ind. Eng. Chem. Res.* **2002**, *41*, 5510−5515.
(45) Verevkin, S. P.; Sazonova, A. Y.; Frolkova, A. K.; Zaitsau, D. H.; Prikhodko, I. V.; Held, C. Separation Performance of BioRenewable Deep Eutectic Solvents. *Ind. Eng. Chem. Res.* **2015**, *54* (13), 3498−3504.
(46) Zubeir, L. F.; Held, C.; Sadowski, G.; Kroon, M. C. PC-SAFT Modeling of CO2 Solubilities in Deep Eutectic Solvents. *J. Phys. Chem. B* **2016**, *120* (9), 2300−2310.
(47) Ashworth, C. R.; Matthews, R. P.; Welton, T.; Hunt, P. A. Doubly Ionic Hydrogen Bond Interactions within the Choline Chloride−urea Deep Eutectic Solvent. *Phys. Chem. Chem. Phys.* **2016**, *18* (27), 18145−18160.
(48) Martins, M. A. R.; Carvalho, P. J.; Palma, A. M.; Domańska, U.; Coutinho, J. A. P.; Pinho, S. P. Selecting Critical Properties of Terpenes and Terpenoids through Group-Contribution Methods and Equations of State. *Ind. Eng. Chem. Res.* **2017**, *56* (35), 9895−9905.
(49) Carvalho, P. J.; Regueira, T.; Santos, L. M. N. B. F.; Fernandez, J.; Coutinho, J. A. P. Effect of Water on the Viscosities and Densities of 1-Butyl-3-Methylimidazolium Dicyanamide and 1-Butyl-3-Methylimidazolium Tricyanomethane at Atmospheric Pressure. *J. Chem. Eng. Data* **2010**, *55* (2), 645−652.
(50) Wang, X.; Sun, T.; Teja, A. S. Density, Viscosity, and Thermal Conductivity of Eight Carboxylic Acids from (290.3 to 473.4) K. *J. Chem. Eng. Data* **2016**, *61* (8), 2651−2658.
(51) Cedeño González, F. O.; Prieto González, M. M.; Bada Gancedo, J. C.; Alonso Suárez, R. Estudio de La Densidad y de La Viscosidad de Algunos Ácidos Grasos Puros. *Grasas Aceites* **1999**, *50* (5), 359−368.
(52) Martins, M. A. R.; Neves, C. M. S. S.; Kurnia, K. A.; Carvalho, P. J.; Rocha, M. A. A.; Santos, L. M. N. B. F.; Pinho, S. P.; Freire, M. G. Densities, Viscosities and Derived Thermophysical Properties of Water-Saturated Imidazolium-Based Ionic Liquids. *Fluid Phase Equilib.* **2016**, *407*, 188−196.
(53) Okoturo, O. O.; VanderNoot, T. J. Temperature Dependence of Viscosity for Room Temperature Ionic Liquids. *J. Electroanal. Chem.* **2004**, *568*, 167−181.
(54) Florindo, C.; McIntosh, A. J. S.; Welton, T.; Branco, L. C.; Marrucho, I. M. A Closer Look into Deep Eutectic Solvents: Exploring Intermolecular Interactions Using Solvatochromic Probes. *Phys. Chem. Chem. Phys.* **2018**, *20* (1), 206−213.
(55) Yalkowsky, S. H.; He, Y.; Jain, P. *Handbook of Aqueous Solubility Data*, 2nd ed.; CRC Press, 2010.

DOI: 10.1021/acssuschemeng.8b01203
ACS Sustainable Chem. Eng. XXXX, XXX, XXX−XXX